




## Article

# Fe@Hierarchical BEA Zeolite Catalyst for MW-Assisted Alcohol Oxidation Reaction: A Greener Approach

Marta A. Andrade <sup>1</sup>, Leonardo M. S. Ansari <sup>1,2</sup>, Armando J. L. Pombeiro <sup>1</sup>, Ana P. Carvalho <sup>3</sup>, Angela Martins <sup>2,3,\*</sup> and Luísa M. D. R. S. Martins <sup>1,\*</sup>

<sup>1</sup> Centro de Química Estrutural and Departamento de Engenharia Química, Instituto Superior Técnico, Universidade de Lisboa, 1049-001 Lisboa, Portugal; marta.andrade@tecnico.ulisboa.pt (M.A.A.); A39206@alunos.isel.pt (L.M.S.A.); pombeiro@tecnico.ulisboa.pt (A.J.L.P.)

<sup>2</sup> Área Departamental de Engenharia Química, Instituto Superior de Engenharia de Lisboa, IPL, 1959-007 Lisboa, Portugal

<sup>3</sup> Centro de Química Estrutural and Departamento de Química e Bioquímica, Faculdade de Ciências, Universidade de Lisboa, 1749-016 Lisboa, Portugal; ana.carvalho@ciencias.ulisboa.pt

\* Correspondence: amartins@deq.isel.ipl.pt (A.M.); luisammartins@tecnico.ulisboa.pt (L.M.D.R.S.M.); Tel.: +351-218419389 (L.M.D.R.S.M.)

Received: 10 August 2020; Accepted: 2 September 2020; Published: 8 September 2020



**Abstract:** The aim of this study was to investigate the catalytic activity of hybrid materials of iron supported on hierarchical zeolites in the oxidation reaction of 1-phenylethanol to acetophenone. A greener approach was considered for the preparation of the catalyst and performance of the oxidation reaction. Hierarchical BEA zeolite samples were obtained from an alkaline and a subsequent acid treatment. The materials were characterized by X-ray diffraction (XRD), transmission electron microscopy (TEM) and nitrogen adsorption at  $-196\text{ }^{\circ}\text{C}$ . An iron salt was incorporated onto the hierarchical zeolites by mechanochemical grinding and the catalytic performance of the prepared materials was evaluated towards the microwave assisted oxidation reaction of 1-phenylethanol. The catalyst obtained by Fe immobilization on sample modified by 0.2 M NaOH followed by acid treatment (Fe@BEA0.2AT) is the most promising material with 35% yield and 56% selectivity to acetophenone, allowing five reuse cycles without significant loss of activity and selectivity.

**Keywords:** hierarchical BEA zeolite; mechanochemical grinding; iron; microwave-assisted oxidation; heterogeneous catalysis; secondary alcohol

## 1. Introduction

The selective oxidation of alcohols to targeted carbonyl-containing compounds is among the central reactions in organic chemistry, with a pivotal role at industrial level, attracting a great attention for the development of environmentally friendly processes and sustainable production of novel materials and energy sources [1–3].

Even though some remarkable advances have been accomplished, only a few known catalytic systems are able to offer both economic and practical oxidation approaches toward industrially significant transformations. Many of the found methods present several drawbacks, as high reagent cost, instability, use of hazardous metals or oxidants, harsh reaction conditions, operational complexity, low selectivity and low yields, requirement of additives/co-catalysts, or huge production of wastes [3]. Regarding the catalyst, synthetic limitations have also been encountered, with their synthesis involving considerable work (multiple steps) and limited yields. To overcome such challenges, there is a continuing pursuit for innovative catalytic systems.

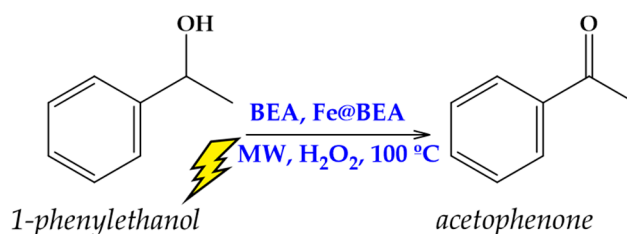
Zeolites are inorganic catalysts with a wide range of applications, especially in refining and petrochemistry processes, as well as with some emerging utilizations as catalysts or catalyst supports in reactions that usually occur in the presence of environmentally unfriendly homogeneous catalysts [4]. To overcome the intrinsic microporosity of zeolites that hamper their application in the presence of large molecules, additional porosity in the mesopore range can be created through several methods. Desilication is a simple and low-cost post-synthesis method consisting in an alkaline treatment using organic or inorganic bases, with NaOH being the most used [5,6]. Since this procedure generally leads to the deposition of extra-framework debris that can lead to partial occlusion of the pores, an additional acid treatment is recommended to unblock the access to the internal porosity of the zeolite [7].

Desilicated zeolites have been used as supports for metal complexes immobilization [8] and metals [9,10] for diverse reactions, involving most of the times a conventional immobilization method of the metal salt in solution. Some recent studies have reported the mechanochemical preparation of iron-immobilized species onto desilicated ZSM-5 zeolites and their application in selective microwave-assisted oxidation reactions [9,10].

Mechanochemistry is one of the most suitable alternative routes to catalyst conventional preparation procedures due to its simplicity and high reproducibility [11]. This methodology is also environmentally friendly, providing solvent-free, mild reaction conditions and short reaction times. The use of microwave (MW) irradiation has also drawn much attention in synthetic organic chemistry due to reported efficiency and selectivity improvement, faster reaction rates, as well as energy saving. This technology can therefore be considered as a valuable alternative energy source in organic synthesis, presenting an environmentally friendly nature [3,12–15].

The use of MW irradiation and mechanochemistry represents a simple alternative to conventionally adopted synthetic protocols to obtain novel and efficient catalysts, in contrast to established conventional approaches, which generally involve complex processes, heating and/or the addition of costly and/or harmful chemicals.

In an attempt to point for a greener approach, overcoming some of the above-mentioned disadvantages of alcohol oxidation processes, the current work aimed at developing a catalytic system for efficient and selective conversion of secondary alcohols to the corresponding ketones under relatively mild conditions, based on the use of cheap and commercially available simple metal chloride catalysts. Herein, we report the oxidation of 1-phenylethanol to acetophenone, as a well-known model reaction, by aqueous hydrogen peroxide using Fe immobilized in hierarchical BEA zeolites, without the need for any additive (Scheme 1). The used procedure highlights the advantages of mechanochemistry for the preparation of the catalysts and the use of MW-irradiation on the catalytic oxidation of 1-phenylethanol. Overall, a more sustainable protocol was followed, allowing energy and time saving of the overall process.



**Scheme 1.** MW-assisted oxidation of 1-phenylethanol to acetophenone with hydrogen peroxide catalyzed by BEA and Fe@BEA materials.

## 2. Results and Discussion

BEA zeolite was modified through alkaline treatments followed by an acid treatment. Parent and modified samples were functionalized with an iron salt ( $\text{FeCl}_2 \cdot 4\text{H}_2\text{O}$ ) incorporated by ball milling.

The materials were tested as catalysts under microwave-assisted irradiation towards the oxidation of 1-phenylethanol.

The X-ray powder diffraction patterns of the starting material and modified samples, as well as immobilized catalysts (Figure 1), reveal the characteristic peaks of zeolite BEA [16] showing that the long-range crystal ordering is preserved upon alkaline and acid treatments, and is not affected by the mechanical gridding since no important change in the position of the most intense peak, at  $2\theta$  around  $22^\circ$ , is observed. On the contrary, a considerable broadening of the peak occurs upon the modification treatments, and also after iron immobilization, suggesting the occurrence of some destruction of the crystals, resulting in smaller crystallites (see the values of the full width at half maximum quoted in Table 1).

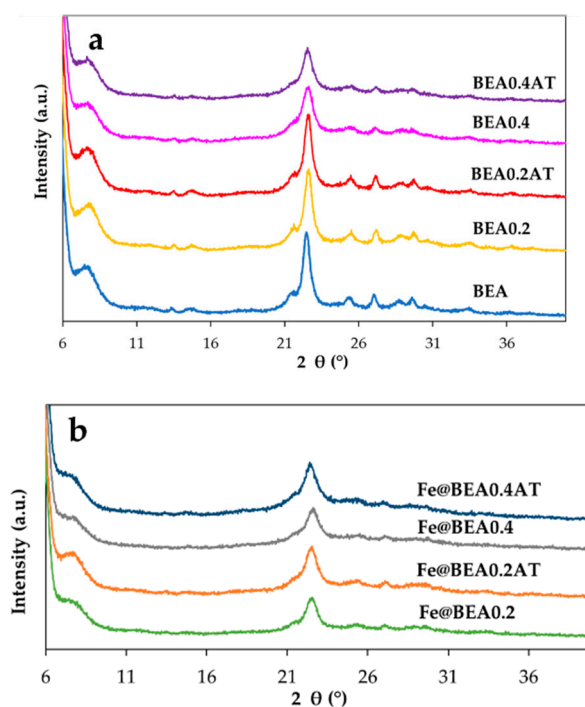


**Figure 1.** X-ray diffraction patterns of (a) parent and modified BEA samples, and (b) immobilized Fe catalysts. For the samples' designations, see the Materials and Methods section.

**Table 1.** Full width at half maximum (FWHM) of diffraction peak at  $22^\circ$   $2\theta$ , degree of crystallinity ( $C_{XRD}$ ) and mass loss values. Values in brackets were estimated taking as reference the modified sample prior to acid treatment or Fe immobilization.

Sample	FWHM ( $^\circ 2\theta$ )	$C_{XRD}$ (%)	Mass Loss (%)
BEA	0.65	100	-
BEA0.2	0.70	87	13.1
BEA0.2AT	0.70	90 (100)	19.4 (6.3)
BEA0.4	1.00	76	24.5
BEA0.4AT	1.00	74 (98)	43.1 (18.6)
Fe@BEA0.2	1.10	56 (65)	-
Fe@BEA0.2AT	1.10	65 (72)	-
Fe@BEA0.4	1.30	57 (76)	-
Fe@BEA0.4AT	1.30	55 (74)	-

The diffraction patterns allowed the determination of the percentage of crystallinity,  $C_{XRD}$ , of the modified samples based on the area of the peak at  $2\theta$  of around  $22^\circ$ , measured using Peak Fit software. Besides the common estimation taking the parent BEA sample as reference, values considering as

reference the modified sample prior to acid treatment, or Fe immobilization, were also determined and presented on Table 1 in brackets.

The crystallinity and mass loss values presented in Table 1 show that the basic treatment had a more structural destructive effect in the case of sample BEA0.4, which only retained 76% of the  $C_{XRD}$  of the starting material, which correlates with its higher mass loss when compared with that observed for BEA0.2 (13.1% vs. 24.5%). The subsequent acid treatment had no impact on the samples crystallinity as shown by the values in brackets, which allows to evaluate only the effect of the acid treatment. However, a greater mass loss was observed for sample BEA0.4AT, which may indicate that in this case the acid treatment had a stronger effect resulting in a partial solubilization of the BEA0.4, that is, most certainly, more fragilized due to the higher NaOH concentration used in the desilication treatment.

A loss of crystallinity is also observed when the metal was immobilized by mechanical grinding, due to the fragmentation and partial destruction of the crystal aggregates, in accordance to what was previously stated by Majano et al. [17] and, more recently, by Ferreira et al. [18]. It must be also noted that, despite the different modification conditions, the decrease of crystallinity due to the Fe immobilization procedure is quite close.

The  $N_2$  adsorption–desorption isotherms reproduced in Figure 2 show that the results obtained for starting and modified materials are typical I+IV isotherms [19], disclosing the characteristic micropore network of zeolite structures along with a significant mesopore structure. The presence of mesoporosity in the case of the parent material is interpreted as a result of aggregation of very small particles. The desilication treatment results in a downward deviation of the curves indicating a decrease in micropore volume that is slightly more notorious, as expected, when 0.4 M NaOH solution is used. Upon the acid treatment, some recovery of the microporosity is noted, especially in the case of BEA0.2AT, denoted by an upward deviation of the isotherm, meaning that some unblocking effect of the debris formed as consequence of the alkaline treatment. In the case of BEA0.4AT, this effect is not so visible, most likely because the sample is already fragilized due to the higher base concentration used in the desilication treatment, as indicated by the higher mass and crystallinity loss observed (see Table 1). H4 hysteresis loops are noticed in the isotherms of the modified samples, especially in the case of materials submitted to acid treatment.

Upon the incorporation of the iron salt some blockage of the micropores was observed, pointing out that the Fe species are confined in the microporosity of the zeolite, as corroborated by the absence of black spots characteristic of metal particles immobilized at the external surface of the crystals in the transmission electron microscopy (TEM) images. Concurrently, an increase of the mesopore volume was also noticed, that can be ascribed to the ball milling technique used for the immobilization of Fe. As previously mentioned, the Mechanical grinding could lead to some disaggregation of the small crystal aggregates of treated BEA, causing some occlusion of the microporosity and, simultaneously, increasing the intercrystalline mesoporosity.

In line with the previous discussion, the textural parameters reported in Table 2 reveal that the modification treatments resulted in the decrease of the micropore volume,  $V_{micro}$ , always more pronounced when 0.4 M NaOH was used in the desilication step. The development of mesoporosity is also evident, being more important upon the acid treatment, as expected. Actually, while for the desilicated samples the mesopore volume,  $V_{meso}$  presents an increase of only 5–7%, for the samples obtained after the acid washing the values reach 20–22%, along with some increase of  $V_{micro}$  values.

The mesopore distributions (Figure 2, right side) were obtained through Hybrid Density Functional Theory (DFT Plus (R) V2.01 for ASAP 2010 V5.00 assuming cylindrical pores. Overall, modified samples as well as the pristine zeolite present broad mesopore size distributions and the large majority of pore widths fall in the region 10–40 nm. On the other hand, a closer examination highlights that while for BEA0.2 and BEA0.2AT, the distribution is very similar to BEA, in the case of BEA0.4 and BEA0.4AT, there is an evident difference on the volume of mesopores, when compared to BEA, or BEA0.2, and an accentuated increase in the pores with width in the region between 10 to 20 nm.

In the case of sample Fe@BEA0.2, a wider pore width distribution can be observed, starting at lower values, from around 7 nm.

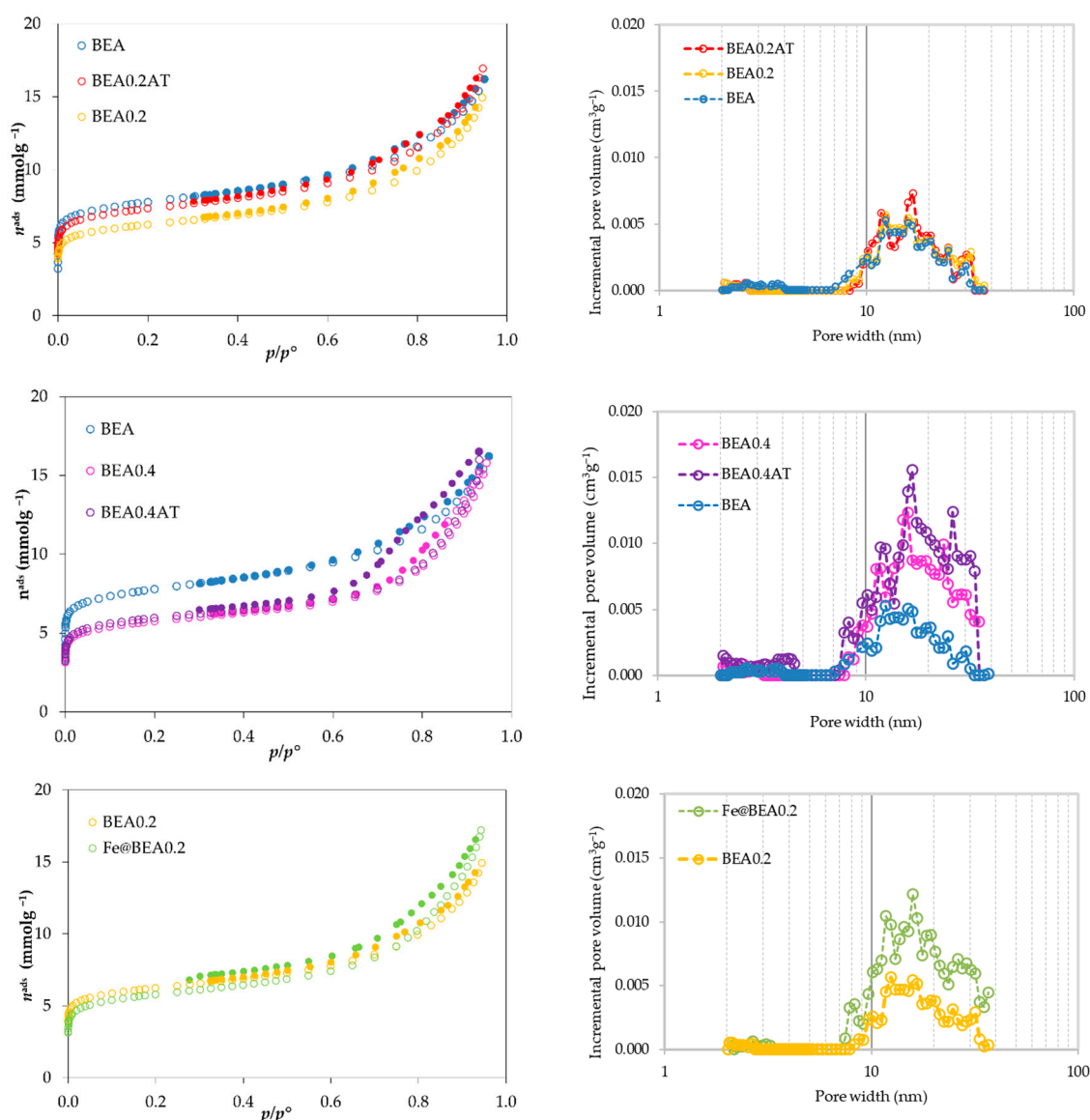


**Figure 2.** N<sub>2</sub> adsorption-desorption isotherms obtained at −196 °C (left side) and mesopore size distributions (right side).

**Table 2.** Textural parameters of selected samples obtained from the N<sub>2</sub> adsorption isotherms at −196 °C.

Sample	$V_{\text{micro}}^a$ (cm <sup>3</sup> g <sup>−1</sup> )	$V_{\text{meso}}^b$ (cm <sup>3</sup> g <sup>−1</sup> )	$V_{\text{total}}^c$ (cm <sup>3</sup> g <sup>−1</sup> )	$A_{\text{ext}}$ (m <sup>2</sup> g <sup>−1</sup> )
BEA	0.17	0.40	0.57	246
BEA0.2	0.13	0.42	0.52	211
BEA0.2AT	0.15	0.49	0.59	237
BEA0.4	0.12	0.43	0.55	191
BEA0.4AT	0.13	0.48	0.58	190
Fe@BEA0.2	0.09	0.51	0.60	234
Fe@BEA0.2AT	0.10	0.50	0.60	225

<sup>a</sup>  $V_{\text{micro}}$ , was evaluated applying the  $\alpha_5$  method taking as reference the isotherm obtained for a non-porous silica [20];

<sup>b</sup>  $V_{\text{meso}}$ , calculated between the  $V_{\text{total}}$  and  $V_{\text{micro}}$ ; <sup>c</sup>  $V_{\text{total}}$ , considered as the N<sub>2</sub> uptake at  $p/p^0 = 0.95$ .

The mechanochemistry methodology was effective in the incorporation of Fe amounts close to the theoretical loadings (0.3–0.6 wt.%) and the determined Fe content is shown in Table 3.

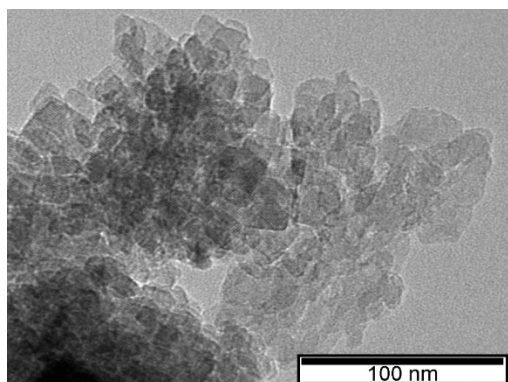
**Table 3.** Iron loadings obtained after heterogenization of the iron salts on the different zeolite materials.

Catalyst	Fe (% wt)
Fe@BEA	0.36
Fe@BEA0.2	0.38
Fe@BEA0.2AT	0.54
Fe@BEA0.2AT (5th cycle)	0.09
AF@BEA0.4	0.36
Fe@BEA0.4AT	0.46

Figure 3 shows TEM images of samples Fe@BEA and Fe@BEA0.2AT, in the case of this last one, the fresh catalyst as well as that recovered after five catalytic cycles are shown. The TEM images of the Fe@BEA denote the presence of aggregates made of very small crystals, typical of BEA zeolite, with well-defined contours. On the other hand, for Fe@BEA0.2AT zeolite (Figure 3b) it is notorious that the crystal edges are more irregular due to the alkaline + acid washing treatments that caused some “corrosion” of external surface of the crystals. However, upon the 5th catalytic cycle, the appearance of the crystals was kept unchanged, as expected, attending to the mild experimental conditions used during the catalytic essays. It is worth mentioning that despite the presence of Fe on all samples was quantified (see Table 3), it was very difficult to visualize the Fe particles dispersed on the zeolitic support, which can be attributed to two reasons: the small amount of Fe introduced and the preferential location inside the zeolite pores, attending to the small dimension of Fe that can fit the zeolite micropores.

The starting and supported materials were investigated as catalysts for the oxidation of 1-phenylethanol under previously optimized microwave irradiation conditions, using hydrogen peroxide as oxidant (30% aqueous solution) and the solvent acetonitrile (MeCN). The choice of hydrogen peroxide as oxidizing agent was based on its good performance as an oxidant in this reaction and on its reduced environmental impact, since it produces only water as a by-product. Acetonitrile was chosen as solvent, due to its high resistance to the oxidizing agent. Microwave irradiation was chosen on the basis of previously reported results [3,20–22] and given its advantages in delivering a more efficient and faster process, when compared to conventional heating.

Results obtained for the different investigated catalysts towards 1-phenylethanol oxidation are summarized in Table 4 and Figure 4. The catalytic performance of the hybrid materials was evaluated in terms of products yield, turnover number (TON) or frequency (TOF,  $\text{h}^{-1}$ ), and selectivity to acetophenone.



(a)

**Figure 3.** Cont.



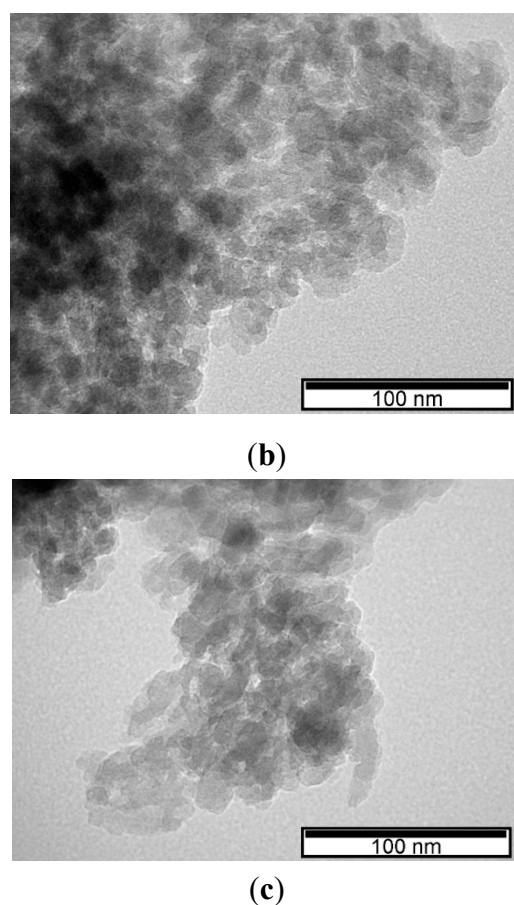


**Figure 3.** TEM images of Fe@BEA (a), Fe@BEA0.2AT (b), and Fe@BEA0.2AT (5th cycle) (c).

**Table 4.** Microwave-assisted catalytic oxidation of 1-phenylethanol with  $\text{H}_2\text{O}_2$  in MeCN, catalyzed by Fe@zeolite materials (selected data) <sup>a</sup>.

Catalyst	Acetophenone Yield (%) <sup>b</sup>	TON <sup>c</sup>	TOF ( $\text{h}^{-1}$ )	Selectivity <sup>d</sup> to Acetophenone (%)
BEA <sup>e</sup>	9	-	-	27
BEA0.2 <sup>e</sup>	11	-	-	29
BEA0.2AT <sup>e</sup>	10	-	-	28
Fe@BEA	20	366	439	46
Fe@BEA0.2	28	495	594	52
Fe@BEA0.2AT	35	430	516	53
Fe@BEA0.4	15	221	265	32
Fe@BEA0.4AT	34	386	463	66
Fe <sup>e</sup>	19	315	378	21
- <sup>f</sup>	3	-	-	-

<sup>a</sup> Reaction conditions (unless stated otherwise): MW (25 W), acetonitrile (2.0 mL), 1-phenylethanol (1.65 mmol),  $\text{H}_2\text{O}_2$  (30% aq. sol., 3.12 mmol), Fe (1  $\mu\text{mol}$ ), 50 min, 100 °C; <sup>b</sup> Molar yields based on substrate determined by gas chromatographic (GC) analysis, i.e., moles of product (acetophenone) per 100 mol of 1-phenylethanol; <sup>c</sup> Turnover number (moles of product per mol of supported catalyst) determined by GC analysis. <sup>d</sup> Moles of desired product per mol of converted 1-phenylethanol; <sup>e</sup>  $\text{FeCl}_2 \cdot 4\text{H}_2\text{O}$ ; <sup>f</sup> 30 min.

The results in Table 4 and Figure 4 show that the parent and treated zeolites present some catalytic activity, in line to what was previously reported in the literature [9,10]. The catalytic activity of the pristine support in the MW-assisted oxidation of 1-phenylethanol revealed an acetophenone yield of 9%, which is kept almost constant upon zeolite treatments. Given this similar catalytic behavior for the parent and treated zeolites, it is assumed that hypothetical changes in the acidity of the samples would

not be of significance in this study. However, a considerable increase of the catalytic activity is observed upon the introduction of Fe in the modified BEA samples, achieving acetophenone yields up to three times as high, for the hybrid catalysts, with a significant selectivity enhancement. Acetophenone was obtained with selectivities above 50% with yields between 33% to 35% of 1-phenylethanol under mild reaction conditions and a relatively short reaction time (50 min). An increase of the reaction time was not significant for improved acetophenone yield in these systems, which remained in the 30–35% range. Moreover, this simple catalytic system using only 0.1% mol of catalyst when compared to the substrate, could provide high TON values (up to ca. 600) comparing favorably to other systems reported in the literature [21–25].

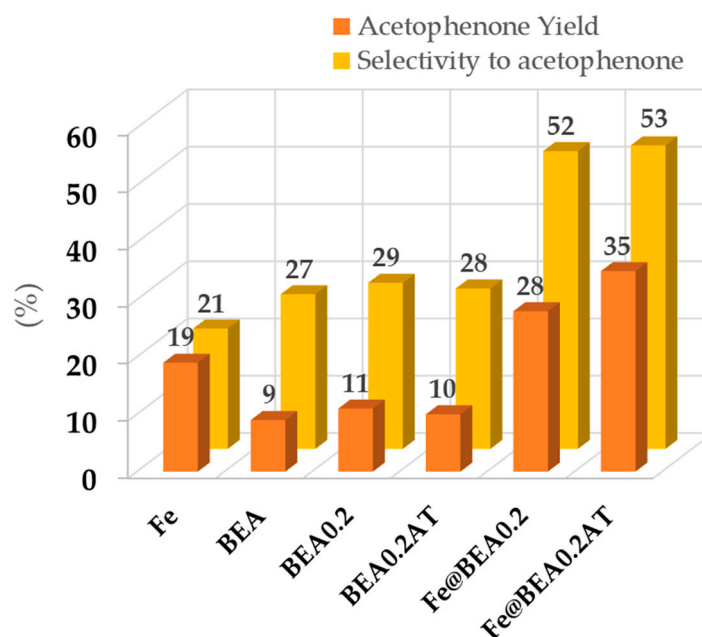


**Figure 4.** Acetophenone yield and selectivity for the MW-assisted oxidation of 1-phenylethanol over the selected catalysts.

The enhanced catalytic activity of Fe immobilized hierarchical zeolites over their parent zeolites could be related to their textural characteristics that can impose more or less important diffusional constraints to 1-phenylethanol to access the active sites. Thus, an increase in mesoporosity can lead to a higher accessibility of the substrate to Fe anchored at the internal pores of the zeolite sample. The development of mesoporosity has therefore shown to have positive effects on the reaction yield, especially for samples subjected to an alkaline and acid treatment. The crystallinity decrease of the sample Fe@BEA0.2AT (65%) does not seem to have a significant influence in the catalytic activity. On the other hand, for the samples treated with 0.4 M NaOH, a distinct behavior is observed. In the case of Fe@BEA0.4 catalyst, a significant decrease in acetophenone yield and selectivity is observed that can be attributed to a higher accumulation of debris at the pore mouth of the zeolite, formed during the desilication treatment, causing more accentuated diffusional limitations, thus hindering the access of the reactants to the active sites. On the other hand, for sample Fe@BEA0.4AT, the unblocking of the pores through the acid treatment as well as the ball milling process, originates a highly fragile structure that can no longer efficiently retain the Fe particles and the occurrence of leaching is observed already on the first catalytic cycle. Thus, despite the relatively high yield and selectivity, the catalytic system behaves as a mixture of heterogeneous + homogeneous systems.

Regarding selectivity, and under the above optimized conditions, besides acetophenone, benzoic acid, 1-(1-phenyl-ethoxy)-ethylbenzene and 1-phenylethyl formate were also detected by GC-MS analysis. The homogeneous catalytic reaction was performed using the non-supported iron salt



$\text{FeCl}_2 \cdot 4\text{H}_2\text{O}$  and a lower yield of 19% was obtained, also with an inferior value for selectivity to acetophenone (21%) when compared to the supported systems. Therefore, considering the catalytic results, a synergism between the modified zeolites and Fe is observed in each case, given the higher acetophenone yields obtained for the Fe-immobilized materials, when compared to BEA and the iron salt alone.

In order to evaluate the advantages of using microwave radiation as a heating source, an oxidation reaction using Fe@BEA0.2AT as catalyst, was performed under the same reaction conditions in a round bottom flask but using an oil bath as heating source. The yield of acetophenone obtained in this case was of 9%, which compares rather unfavorably to the 35% obtained for the MW-assisted reaction. The higher efficacy of the MW-assisted reaction arises from the efficient internal heating by direct coupling of microwave energy with the molecules (solvents, reagents, catalyst) in the reaction mixture [12–15]. The uniform temperature increase throughout the sample results in minimized wall effects, which can lead to the occurrence of the alleged specific microwave effects. Comparatively, conventional heating with an external heat source is a slow and inefficient process for energy transfer into the system, relying on convection currents and on thermal conductivity of the materials, leading to a temperature gradient, with a higher temperature of the reaction vessel than that of the reaction mixture, that ultimately can result in product, substrate, or reagent decomposition.

In this study, the ability to reuse the spent catalysts was evaluated over several consecutive cycles. The catalysts Fe@BEA and Fe@BEA0.2AT were therefore subjected to five consecutive reactions (Figure 5). For the iron immobilized in the commercial zeolitic support, Fe@BEA, a sharp drop of more than 50% of the acetophenone yield is observed after the first cycle, while maintaining the yield in the third and fourth cycles. The significant loss of activity from the first to the second cycle pointed out the lack of stability of this material and was a reason why Fe leaching was not further investigated in this case.

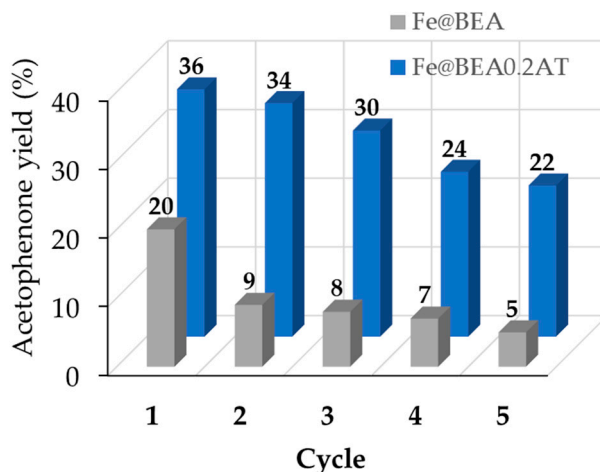


**Figure 5.** Effect of the number of cycles on the acetophenone yield of the MW-assisted 1-phenylethanol oxidation reaction catalyzed by Fe supported on zeolite BEA and BEA0.2AT.

In the case of sample Fe@BEA0.2AT, the best performing catalyst, a higher stability is shown in the first cycles, as a result of the modification treatment of BEA. The yield decreases only in the third cycle, being more accentuated in the fourth cycle, when an overall drop of 33% is observed. After the 5th cycle, the catalysts maintain a quarter of its initial activity. These results are related to iron leaching to the solution, as assessed by inductively coupled plasma (ICP) atomic emission spectroscopy at the end of the fifth cycle (83%). Nevertheless, an increase of the selectivity to acetophenone was observed after each cycle, reaching 84% in the fifth cycle.

### 3. Materials and Methods

In this study, commercially-available chemicals were used without further purification. The parent material for this work was the commercial zeolite BEA (Lot. CP814E, from Zeolyst Farmsum, Netherland) with Si/Al molar ratio = 12.5, supplied as  $\text{NH}_4\text{BEA}$  and transformed into the protonic form through calcination under dry air ( $6 \text{ L h}^{-1}\text{g}^{-1}$ ) at  $500^\circ\text{C}$  for 3 h.

#### 3.1. Preparation of the Hierarchical BEA Zeolite Samples

Desilicated samples were obtained according to procedures described in the literature [5,6] in which the zeolite in its protonic form, herein designated as BEA was treated with 100 mL of solutions with 0.2 or 0.4 M NaOH (Merck, p.a., Darmstadt, Germany), using a liquid:solid proportion of  $30 \text{ mL g}^{-1}$  for 30 min at  $60^\circ\text{C}$ , with vigorous stirring. The resulting material was recovered by centrifugation, thoroughly washed, and dried. To account for some Na exchange during the alkaline treatment, the desilicated samples were reconverted to the protonic form by ion exchange, with a 1 M  $\text{NH}_4\text{NO}_3$  (Merck, p.a., Darmstadt, Germany) solution, using a liquid:solid relation of  $25 \text{ mL g}^{-1}$ , at  $80^\circ\text{C}$ , for 6 h. The solid was recovered by centrifugation, dried and calcinated at  $500^\circ\text{C}$  for 3 h under dry air ( $6 \text{ L h}^{-1}\text{g}^{-1}$ ). The desilicated samples were further treated with a 0.1 M HCl (Merck, p.a. fuming 37%, Darmstadt, Germany) solution with a liquid:solid ratio of  $30 \text{ mL g}^{-1}$ , at  $70^\circ\text{C}$ , for 3 h, according to the procedure described in [26]. After centrifugation, the solid was washed, dried, and calcined as described above. The samples were weighed to account for mass loss after each synthesis step. The modified samples will be designated as BEAX, in that X corresponds to the NaOH concentration used in the desilication procedure, followed by AT in the case of samples with the acid treatment.

#### 3.2. Mechanochemical Preparation of Iron Immobilized Materials

The hybrid materials were prepared via a mechanochemical approach. Typically, the zeolite samples were grounded with the target quantity of  $\text{FeCl}_2 \cdot 4\text{H}_2\text{O}$  (Sigma–Aldrich) to achieve a 0.3–0.6 wt% Fe loading in the final material. This procedure was performed using a planetary ball mill (Retsch PM 100 model, Retsch, Haan, Germany) under previously optimized conditions (5 min at 500 rpm). The iron-immobilized materials are designated  $\text{Fe@X}$ , in that “X” is the hierarchical sample.

#### 3.3. Characterization of the Materials

The structural characterization of the parent and modified samples was carried out by X-ray powder diffraction (XRD) (Philips, Almelo, Netherlands) patterns that were obtained at room temperature on an Philips Analytical PW 3050/60 X’Pert PRO with X’Celerator detector, using  $\text{CuK}\alpha$  radiation as incident beam. Diffractograms were obtained by continuous scanning from  $5$  to  $40$  ( $^\circ 2\theta$ ), with a step size of  $0.017^\circ 2\theta$  and time per step of 20 s. The morphological characterization was carried out by Transmission Electron Microscopy (TEM), using a Transmission Electron Microscope Hitachi 8100, with a ThermoNoran light elements EDS detector and digital image acquisition, at Microlab, IST. The textural properties of the materials were assessed by measuring the  $\text{N}_2$  adsorption-desorption isotherms at  $-196^\circ\text{C}$  in an automatic apparatus Micromeritics ASAP 2010 (Micromeritics Instrumets Corporation, Norcross, GA, USA). Before the isotherm measurement, the samples ( $\approx 50 \text{ mg}$ ) were outgassed for 3 h at  $150^\circ\text{C}$  under vacuum better than  $10^{-2} \text{ Pa}$ . The micropore volume,  $V_{\text{micro}}$ , and external area,  $A_{\text{ext}}$ , were assessed by applying the  $\alpha_s$  method using as reference the standard isotherm obtained for a non-porous silica [20]. The micropore volume corresponds to the back extrapolation of the linear region of  $\alpha_s$  plot defined by the experimental points corresponding to  $\alpha_s > 1$  and the external area obtained through the slope. The mesopore pore volume,  $V_{\text{meso}}$ , was estimated from the difference between  $V_{\text{total}}$  and  $V_{\text{micro}}$ , in that  $V_{\text{total}}$  is the total pore volume determined according to the Gurvitch rule, i.e., the amount of  $\text{N}_2$  adsorbed at  $p/p^\circ = 0.95$  [20]. The mesopore size distribution was obtained through Hybrid Density Functional Theory (DFT Plus (R) V2.01 for ASAP 2010 V5.00) assuming cylindrical pores. The iron content present in the immobilized catalysts was analyzed by inductively coupled

plasma (ICP) carried out by Laboratório de Análises, IST using an ICP-AES Horiba Jobin-Yvon model Ultima equipment.

### 3.4. Microwave-Assisted Oxidation of 1-phenylethanol

Catalytic assays were performed using 200  $\mu$ L (1.65 mmol) of 1-phenylethanol, 300  $\mu$ L (3.12 mmol) of hydrogen peroxide (30% aq. sol.), 2 mL of acetonitrile, and 50 mg of catalyst, which were added to 10-mL-capacity cylindrical Pyrex vials with a 13-mm internal diameter. The focused microwave irradiation of the reactional mixture was carried out in an Anton Paar Monowave 300 (Anton Paar GmbH, Graz, Austria) reactor fitted with a rotational system and an IR temperature detector at the desired temperature and reaction time. Blank tests were performed, in iron-free systems, but in the presence of the starting zeolite, and in Fe and zeolite materials free medium. Nitromethane (50  $\mu$ L) was used as internal standard for the gas chromatographic (GC) analyses. After the reaction, the mixture was cooled to room temperature and the suspension (due to the supported catalyst) was centrifuged and filtrated to prepare the samples for GC analysis. The reaction products were analyzed in a Fisons Instruments GC 8000 series (Fisons Instruments, Loughborough, UK) gas chromatograph equipped with a Flame Ionization Detector and a capillary column (DB-WAX, column length: 30 m; internal diameter: 0.32 mm, SGE Analytical Science Europe Ltd, Milton Keynes, UK) and run by the software Jasco-Borwin v.1.50. He was used as the carrier gas. The temperature of injection was 240 °C. The initial temperature, 120 °C, was maintained for 1 min, then increased by 10 °C per min until 200 °C and held for 1 min. The total time of analysis was 10 min. The ionization voltage was 70 eV. GC-MS analyses were performed by using a PerkinElmer Clarus 600 C (Shelton, CT, USA) instrument (He as the carrier gas), equipped with two capillary columns (SGE BPX5; 30 mV0.32 mmV25 mm (SGE Analytical Science Europe Ltd, Milton Keynes, UK), one having an EI-MS (electron impact) detector and the other one with an FID detector. Reaction products were identified by comparing their retention times with known reference compounds, and their mass spectra to fragmentation patterns obtained from the NIST spectral library stored in the computer software of the mass spectrometer.

### 3.5. Recycling Assays

Recyclability of the catalysts was investigated through the reuse in consecutive cycles. A new cycle was initiated after the previous one, with addition of new typical portions of all reagents. The reaction products were analyzed as mentioned above after completion of each run and catalyst recovery was achieved by filtration, followed by washing with acetonitrile, and drying overnight in an oven at 50 °C. Iron leaching from the catalyst was assessed after the 5th catalytic cycle throughout the determination of the iron content of the retrieved solid by ICP.

## 4. Conclusions

This study aimed to contribute to the development of the preparation of zeolite-supported catalysts. The focus was on the optimization of the experimental conditions used for the preparation of modified zeolites to support Fe species, through mechanochemical immobilization, in order to oxidize 1-phenylethanol to acetophenone using microwave radiation as a heating source.

Zeolite BEA was subjected to an alkaline treatment with different NaOH concentrations followed by acid treatment. Hierarchical materials were obtained as evidenced by an increase in the mesoporous volume, without significant loss of crystallinity, especially for the sample treated with 0.2 M NaOH. Upon functionalization with Fe, introduced by ball milling, the hybrid hierarchical materials showed improved catalytic performance in 1-phenylethanol oxidation for the Fe@BEA0.2AT sample, without significant yield losses for more than three consecutive cycles.

This innovative yet simple catalytic system uses alternative green methodologies for the preparation of the catalysts and their performance in a catalytic oxidation reaction. In light of the results obtained, catalysts obtained from Fe immobilization on modified zeolites deserve further investigation for catalytic applications.

**Author Contributions:** Conceptualization, A.M. and L.M.D.R.S.M.; investigation, L.M.S.A., A.P.C., and M.A.A.; writing—original draft preparation M.A.A.; writing—review and editing, M.A.A., A.P.C., A.M., A.J.L.P., and L.M.D.R.S.M.; supervision, A.M. and L.M.D.R.S.M.; funding acquisition, A.P.C., A.M., A.J.L.P., and L.M.D.R.S.M. All authors have read and agreed to the published version of the manuscript.

**Funding:** This research was partially funded by Fundação para a Ciência e a Tecnologia through UIDB/00100/2020 project of Centro de Química Estrutural. M.A.A. acknowledges financial support from UID/QUI/00100/2019-BL/CQE-2017-022 FCT grant.

**Conflicts of Interest:** The authors declare no conflict of interest.

## References

1. Paterson, S. Alcohol Oxidation: Reaction. In *Effects and Applications*; Nova Science Publishers Inc.: New York, NY, USA, 2018.
2. Corberán, V.C.; González-Pérez, M.; Martínez-González, S.; Gómez-Avilés, A. Green oxidation of fatty alcohols: Challenges and opportunities. *Appl. Catal. A Gen.* **2014**, *474*, 211–223. [[CrossRef](#)]
3. Kopylovich, M.N.; Ribeiro, A.P.; Alegria, E.C.; Martins, N.M.R.; Martins, L.M.; Pombeiro, A.J.L. Catalytic Oxidation of Alcohols. In *Advances in Organometallic Chemistry*; Elsevier Inc.: Amsterdam, The Netherlands, 2015; Volume 63, pp. 91–174.
4. Sheldon, R.A.; van Bekkum, H. *Fine Chemicals Through Heterogeneous Catalysis*; Wiley-VCH Verlag GmbH & Co.KGaA: Weinheim, Germany, 2008.
5. Paixão, V.; Carvalho, A.P.; Rocha, J.; Fernandes, A.; Martins, A.B. Modification of MOR by desilication treatments: Structural, textural and acidic characterization. *Microporous Mesoporous Mater.* **2010**, *131*, 350–357. [[CrossRef](#)]
6. Groen, J.C.; Abelló, S.; Villaescusa, L.A.; Pérez-Ramírez, J. Mesoporous beta zeolite obtained by desilication. *Microporous Mesoporous Mater.* **2008**, *114*, 93–102. [[CrossRef](#)]
7. Verboekend, D.; Mitchell, S.; Milina, M.; Groen, J.C.; Pérez-Ramírez, J. Full Compositional Flexibility in the Preparation of Mesoporous MFI Zeolites by Desilication. *J. Phys. Chem. C* **2011**, *115*, 14193–14203. [[CrossRef](#)]
8. Martins, L.M.; Martins, A.B.; Alegria, E.C.; Carvalho, A.P.; Pombeiro, A.J.L. Efficient cyclohexane oxidation with hydrogen peroxide catalysed by a C-scorpionate iron (II) complex immobilized on desilicated MOR zeolite. *Appl. Catal. A Gen.* **2013**, *464*, 43–50. [[CrossRef](#)]
9. Grau-Atienza, A.; Campos, R.; Serrano, E.; Ojeda, M.; Romero, A.A.; García-Martínez, J.; Luque, R. Insights into the Active Species of Nanoparticle-Functionalized Hierarchical Zeolites in Alkylation Reactions. *ChemCatChem* **2014**, *6*, 3530–3539. [[CrossRef](#)]
10. Ojeda, M.; Grau-Atienza, A.; Campos, R.; Romero, A.A.; Serrano, E.; Marinas, J.M.; García-Martínez, J.; Luque, R. Hierarchical Zeolites and their Catalytic Performance in Selective Oxidative Processes. *ChemSusChem* **2015**, *8*, 1328–1333. [[CrossRef](#)] [[PubMed](#)]
11. Kopylovich, M.N.; Ribeiro, A.P.C.; Alegria, E.C.B.A. Mechanochemical Activation and Catalysis. In *Catalysis Series*; Mahmudov, K.T., Kopylovich, M.N., Guedes da Silva, M.F.C., Pombeiro, A.J.L., Eds.; RCS Publishing: Washington, DC, USA, 2019; Chapter 25, pp. 548–563.
12. Kappe, C. Microwave-Assisted Chemistry. *Compr. Med. Chem. I* **2006**, *3*, 837–860.
13. Rath, A.K.; Gawande, M.B.; Zbořil, R.; Varma, R.S. Microwave-assisted synthesis—Catalytic applications in aqueous media. *Coord. Chem. Rev.* **2015**, *291*, 68–94. [[CrossRef](#)]
14. Ribeiro, A.P.C.; Martins, L.M.D.R.S.; Kuznetsov, M.L.; Pombeiro, A.J.L. Tuning Cyclohexane Oxidation: Combination of Microwave Irradiation and Ionic Liquid with the C-Scorpionate [FeCl<sub>2</sub>(Tpm)] Catalyst. *Organometallics* **2016**, *36*, 192–198. [[CrossRef](#)]
15. Martins, L.M.; Ribeiro, A.; Carabineiro, S.A.C.; Figueiredo, J.L.; Pombeiro, A.J.L. Highly efficient and reusable CNT supported iron (ii) catalyst for microwave assisted alcohol oxidation. *Dalton Trans.* **2016**, *45*, 6816–6819. [[CrossRef](#)] [[PubMed](#)]
16. Treacy, M.; Higgins, J. *Collection of Simulated XRD Powder Patterns for Zeolites*; Elsevier: London, UK, 2001.
17. Majano, G.; Borchardt, L.; Mitchell, S.; Valtchev, V.; Pérez-Ramírez, J. Rediscovering zeolite mechanochemistry—A pathway beyond current synthesis and modification boundaries. *Microporous Mesoporous Mater.* **2014**, *194*, 106–114. [[CrossRef](#)]
18. Ferreira, L.; Ribeiro, M.F.; Fernandes, A.; Martins, A.B. Ball Milling Modified SAPO-11 Based Catalysts for *n*-Decane Hydroisomerization. *ChemistrySelect* **2019**, *4*, 6713–6718. [[CrossRef](#)]

19. Thommes, M.; Kaneko, K.; Neimark, A.V.; Olivier, J.P.; Rodríguez-Reinoso, F.; Rouquerol, J.; Sing, K.S. Physisorption of gases, with special reference to the evaluation of surface area and pore size distribution (IUPAC Technical Report). *Pure Appl. Chem.* **2015**, *87*, 1051–1069. [\[CrossRef\]](#)
20. Gregg, S.J.; Sing, K.S.W. *Adsorption, Surface Area and Porosity*, 2nd ed.; Academic Press: London, UK, 1982.
21. Karmakar, A.; Martins, L.M.; Da Silva, M.F.C.G.; Hazra, S.; Pombeiro, A.J.L. Solvent-Free Microwave-Assisted Peroxidative Oxidation of Alcohols Catalyzed by Iron (III)-TEMPO Catalytic Systems. *Catal. Lett.* **2015**, *145*, 2066–2076. [\[CrossRef\]](#)
22. Ribeiro, A.; Martins, L.M.; Carabineiro, S.A.C.; Buijnsters, J.G.; Figueiredo, J.L.; Pombeiro, A.J.L. Heterogenized C-Scorpionate Iron (II) Complex on Nanostructured Carbon Materials as Recyclable Catalysts for Microwave-Assisted Oxidation Reactions. *ChemCatChem* **2018**, *10*, 1821–1828. [\[CrossRef\]](#)
23. Carabineiro, S.; Martins, L.M.; Pombeiro, A.J.L.; Figueiredo, J.L. Commercial Gold (I) and Gold (III) Compounds Supported on Carbon Materials as Greener Catalysts for the Oxidation of Alkanes and Alcohols. *ChemCatChem* **2018**, *10*, 1804–1813. [\[CrossRef\]](#)
24. Ballarina, B.; Barreca, D.; Boanini, E.; Cassani, M.C.; Dambruoso, P.; Massi, A.; Mignani, A.; Nanni, D.; Parise, C.; Zaghi, A. Supported Gold Nanoparticles for Alcohols Oxidation in Continuous-Flow Heterogeneous Systems. *ACS Sustain. Chem. Eng.* **2017**, *5*, 4746–4756. [\[CrossRef\]](#)
25. Nakamura, K.; Ichikuni, N.; Hara, T.; Kojima, T.; Shimazu, S. The catalytic oxidation of 1-phenylethanol over SiO<sub>2</sub> supported manganese oxide nanocluster prepared by PVP stabilized colloidal Mn as precursor. *Catal. Today* **2020**, *352*, 250–254. [\[CrossRef\]](#)
26. Fernandez, C.; Stan, I.; Gilson, J.-P.; Thomas, K.; Vicente, A.; Bonilla, A.; Pérez-Ramírez, J. Hierarchical ZSM-5 Zeolites in Shape-Selective Xylene Isomerization: Role of Mesoporosity and Acid Site Speciation. *Chem. A Eur. J.* **2010**, *16*, 6224–6233. [\[CrossRef\]](#) [\[PubMed\]](#)



© 2020 by the authors. Licensee MDPI, Basel, Switzerland. This article is an open access article distributed under the terms and conditions of the Creative Commons Attribution (CC BY) license (<http://creativecommons.org/licenses/by/4.0/>).